



# Expansion Light Sheet Microscopy Resolves Subcellular Structures in Large Portions of the Songbird Brain

Daniel Normen Düring<sup>1,2,3\*</sup>†, Mariana Diales Rocha<sup>3†</sup>, Falk Dittrich<sup>3</sup>, Manfred Gahr<sup>3</sup> and Richard Hans Robert Hahnloser<sup>1,2</sup>

<sup>1</sup> Institute of Neuroinformatics, University of Zürich/ETH Zürich, Zurich, Switzerland, <sup>2</sup> Neuroscience Center Zurich (ZNZ), Zurich, Switzerland, <sup>3</sup> Department of Behavioral Neurobiology, Max Planck Institute for Ornithology, Seewiesen, Germany

## OPEN ACCESS

### Edited by:

Laura Batti,  
Wyss Center for Bio and  
Neuroengineering, Switzerland

### Reviewed by:

Marcel Oberlaender,  
CAESAR Zentrum für Fortgeschrittene  
Europäische Wissenschaft und  
Forschung, Germany  
Paolo Bianchini,  
Fondazione Istituto Italiano di  
Tecnologia, Italy  
Edward S. Boyden,  
Massachusetts Institute of  
Technology, United States

### \*Correspondence:

Daniel Normen Düring  
dnd@ini.ethz.ch

†These authors have contributed  
equally to this work

**Received:** 01 October 2018

**Accepted:** 11 January 2019

**Published:** 31 January 2019

### Citation:

Düring DN, Rocha MD, Dittrich F,  
Gahr M and Hahnloser RHR (2019)  
Expansion Light Sheet Microscopy  
Resolves Subcellular Structures in  
Large Portions of the Songbird Brain.  
*Front. Neuroanat.* 13:2.  
doi: 10.3389/fnana.2019.00002

Expansion microscopy and light sheet imaging (ExLSM) provide a viable alternative to existing tissue clearing and large volume imaging approaches. The analysis of intact volumes of brain tissue presents a distinct challenge in neuroscience. Recent advances in tissue clearing and light sheet microscopy have re-addressed this challenge and blossomed into a plethora of protocols with diverse advantages and disadvantages. While refractive index matching achieves near perfect transparency and allows for imaging at large depths, the resolution of cleared brains is usually limited to the micrometer range. Moreover, the often long and harsh tissue clearing protocols hinder preservation of native fluorescence and antigenicity. Here we image large expanded brain volumes of zebra finch brain tissue in commercially available light sheet microscopes. Our expansion light sheet microscopy (ExLSM) approach presents a viable alternative to many clearing and imaging methods because it improves on tissue processing times, fluorophore compatibility, and image resolution.

**Keywords:** expansion microscopy, tissue clearing, songbird, spine morphology, light sheet microscopy, large volume imaging, super resolution microscopy

## INTRODUCTION

Since the advent of modern neuroscience, diverse imaging techniques have allowed us to see the brain's microstructure and have fueled our endeavor to understand its function. With the inherent desire to see even the smallest relevant cellular building blocks, the preservation of detailed topographic information within entire neural circuits becomes challenging. Recent advances demonstrate the feasibility of large volume high-resolution imaging with light (Kleinfeld et al., 2011) or electrons (Kasthuri et al., 2015).

The desire to image entire intact volumes of tissue, a daunting task (Marblestone et al., 2013), is mirrored in the recent explosion of tissue clearing protocols (Richardson and Lichtmann, 2015, 2017).

Clearing protocols strive for deeper light penetration by homogenizing light refraction throughout the sample. These protocols make use of diverse chemical approaches from simple immersion to organic solvent-based delipidation (Susaki and Ueda, 2016). Nearly all clearing protocols sufficiently increase transparency for imaging multiple millimeters deep into tissues. However, targeted fluorescence imaging remains challenging because genetically expressed fluorescent proteins tend to lose their fluorescence and their antigenicity during tissue clearing.

Recent progress in clearing protocols have led to better preservation of fluorescence (CUBIC; Susaki et al., 2015) or to improved post-immunostaining (CLARITY; Chung and Deisseroth, 2013; Tomer et al., 2014 and iDISCO; Renier et al., 2014), but current protocols are either time consuming and/or resource intense, technically challenging, and/or impractical. For excellent overviews, see Richardson and Lichtmann (2015, 2017) and Silvestri et al. (2016), who conclude that no single protocol is superior to all others.

One technique that could address many of the aforementioned shortcomings is expansion microscopy (ExM). In ExM, samples are first incubated with DMSO to introduce acryloyl groups. Then, the proteins (including fluorophores) are cross-linked to a polymer grid. After a protein digestion step, the sample is physically expanded through hyper-hydration (Chen et al., 2016; Chozinski et al., 2016; Tillberg et al., 2016). The increase in resolution resulting from expansion has pushed the limits of confocal microscopy and enabled the investigation of subcellular structures that previously have been difficult to resolve by light microscopy, such as the synaptonemal complex in *Drosophila* (Cahoon et al., 2017). Further, expansion microscopy has proven to be useful in clinical settings by enhancing the resolving power of microscopes (Bucur et al., 2016; Zhao et al., 2017). Although the clearing potential of the expansion protocol and its use for larger specimens have been emphasized (Chen et al., 2015; Richardson and Lichtmann, 2015; Karagiannis and Boyden, 2018), to date ExM has only been applied to tissue samples <200  $\mu\text{m}$  thick from mice and humans.

When large volumes of tissue are to be imaged, preferably with multiple wavelengths, image acquisition times, system stability, and photo bleaching become increasingly problematic (Silvestri et al., 2016). One recent technological revival in fluorescence microscopy, the light sheet microscope, alleviates some of these challenges. By illuminating entire planes of tissue and capturing all image pixels at the same time, imaging is fast and fluorophores show little bleaching (Stelzer, 2015).

Here we combine expansion microscopy of large tissue volumes with light sheet microscopy, termed ExLSM. We demonstrate the feasibility of ExLSM in a small passerine, the zebra finch, and point out some advantages over other clearing methods.

Zebra finches are a well-established model for vocal learning with parallels to human speech acquisition (Bolhuis et al., 2010). Furthermore, the organization of the song system, responsible for song learning and production in songbirds, as an interconnected network of discrete brain nuclei makes it particularly well-suited for the analysis of cerebral sub-volumes (Vicario, 1991). Song system nuclei are known to adapt in response to song learning and practice (Huang et al., 2018), making the application of large tissue ExLSM particularly promising within this field, as discrete nuclei can be dissected and expanded to further analyze connectivity changes in detail. We focus on two nuclei of the song system, HVC (proper name), which drives vocal sequences (Hahnloser et al., 2002) and Area-X, which plays an essential role during vocal learning (Scharff and Nottebohm, 1991).

## METHODS

### Tissue Preparation

Five adult male zebra finches have been intracranially injected into either HVC or Area-X with adeno-associated viruses (AAVs) that express GFP in the cytoplasm of neurons. After isoflurane overdose and transcardial perfusion with phosphate-buffered saline, hemispheres were either sectioned into 60–100  $\mu\text{m}$  thick sections ( $n = 2$  birds) using a microtome (Leica Microsystems, Germany), sectioned into 300–800  $\mu\text{m}$  thick sections containing HVC using a vibratome ( $n = 2$ ), or were handled to surgically remove entire HVCs ( $n = 1$ ).

Animal handling was carried out in accordance with the European Communities Council Directive 2010/63 EU and legislation of the state of Upper Bavaria.

The government of Upper Bavaria, “Sachgebiet 54—Verbraucherschutz, Veterinärwesen, 80538 München” with the record number 55.2-1-54-2532-150-2016 approved animal experiments.

### Expansion and Clearing

We performed the protein retention expansion protocol (proExM) available at [expansionmicroscopy.org](http://expansionmicroscopy.org) with minor modifications to accommodate large tissues. In brief, the activation step needs to be adjusted according to tissue volume. Custom gelation chambers can be constructed by sectioning a 1 ml pipette tip according to size and placing them on a parafilm wrapped object slide for easy handling. Immediately after digestion any movement of the sample should be minimized or avoided. Expansion should be performed in the final imaging container if possible. Large gels can be secured with 3% low melt agarose around the corners of the gel. Small gels or hanging gels can be embedded in 1% low melt agarose. For further details and handling recommendations see **Supplementary Materials**.

### Imaging

Images were acquired in commercially available light sheet microscopes, either the Ultra Microscope II (LaVision Biotec GmbH, Germany) or the Z.1 (Carl Zeiss AG, Germany). Image analysis was performed using Imaris (Bitplane, Great Britain). With exception of the image in **Figure 2F**, which has been deconvolved using Huygens Pro (Scientific Volume Imaging B.V., Netherlands), none of the data has undergone any image preprocessing prior to analysis as is common practice in light based imaging.

## RESULTS

We successfully cleared and expanded adult zebra finch brain tissue of diverse volumes ranging from 60  $\mu\text{m}$  thick sagittal brain sections to [2500  $\times$  2000  $\times$  1200]  $\mu\text{m}^3$  tissue volumes encapsulating an entire HVC (**Figures 1A–F**).

Samples were subsequently imaged in two different light sheet microscopes, first a low-magnification system for overview and integral volume analysis, and, second, a system with a smaller working range but higher magnification.

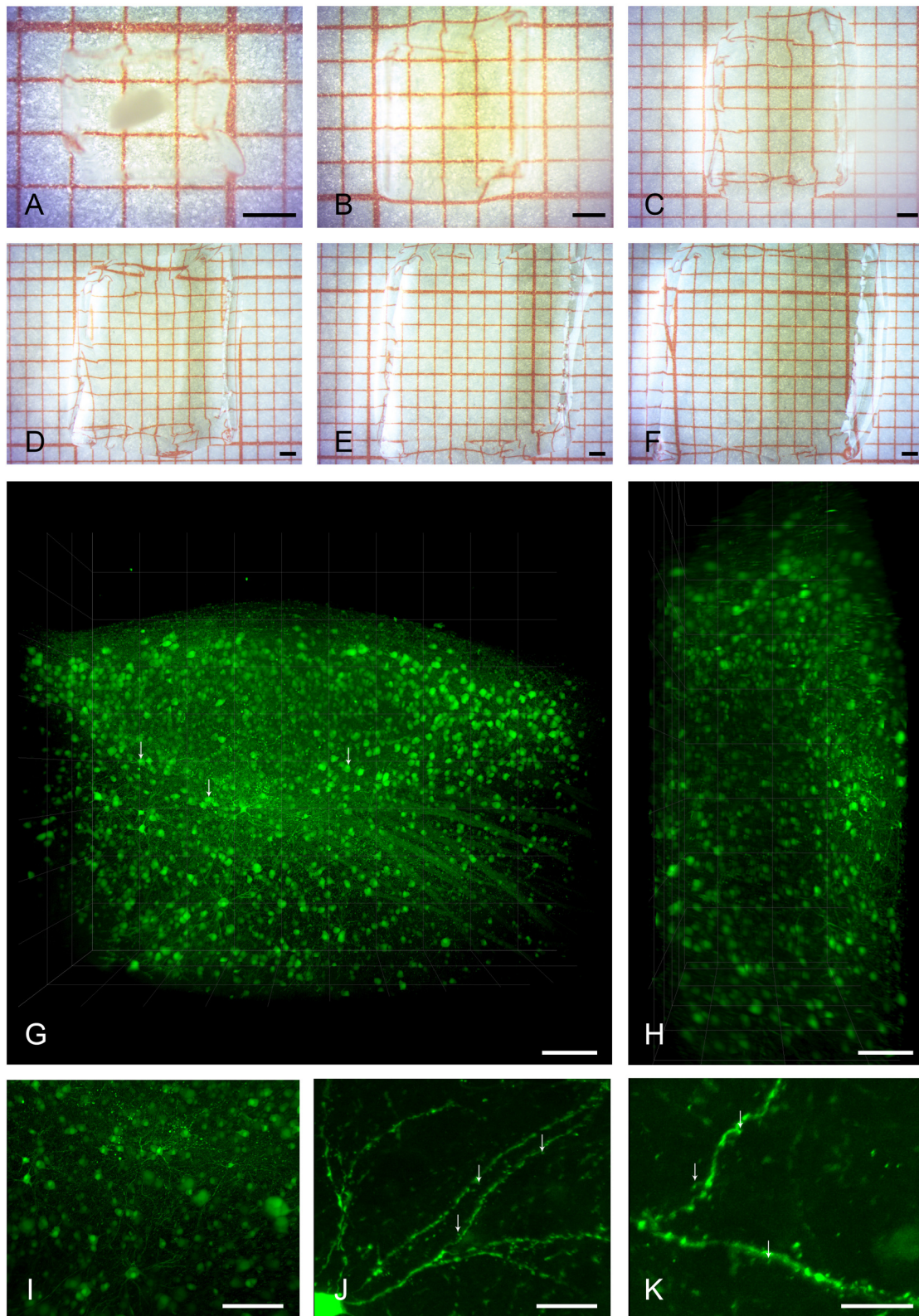


**FIGURE 1** | Clearing, expansion, and imaging of large intact volumes of brain tissue. Top two rows show the typical clearing and swelling progress of the expansion microscopy protocol. A large piece of brain tissue containing HVC is embedded in a polymer gel (A), and is neither expanded nor transparent at this point. Immediately  
(Continued)

**FIGURE 1** | after taking the gel out of the protein digestion solution (**B**), the tissue is already fully transparent and slightly expanded in volume by a factor of two. At this stage, the tissue can be kept in PBS for either imaging, further processing, or storage. Subsequent exchanges of deionized water (**C–F**) lead to a final 4-fold expansion (64 times in volume). Bottom two rows show volume renderings of brain tissue imaged with the LaVision Ultra Microscope II. (**G**) Shows the entire volume of a gel containing a piece of tissue with pre-expansion dimensions of  $[2500 \times 1800 \times 800] \mu\text{m}^3$ , including a large part of HVC. Somata of neurons and even some sub-cellular structures such as nuclei (arrows) are readily visible at a low-magnification setting of 2.5x. Even though the light sheet leads to a slight reduction in axial resolution as seen in the xz-projection view in (**H**), individual neurons can still be discriminated. A digital zoom into the dataset (**I**) reveals some axonal and dendritic processes. The entire dataset was imaged as a single TIFF stack with a z-step size of  $3 \mu\text{m}$ . Imaging at slightly higher magnification of 6.4x allows for the identification of spiny dendrites (arrows, **J,K**). Scale bars (**A–F**) 1 mm, (**G,H**)  $250 \mu\text{m}$ , (**I**)  $150 \mu\text{m}$ , (**J**)  $75 \mu\text{m}$ , (**K**)  $50 \mu\text{m}$ . Scale bars in (**G–K**) correspond to pre-expansion dimensions.

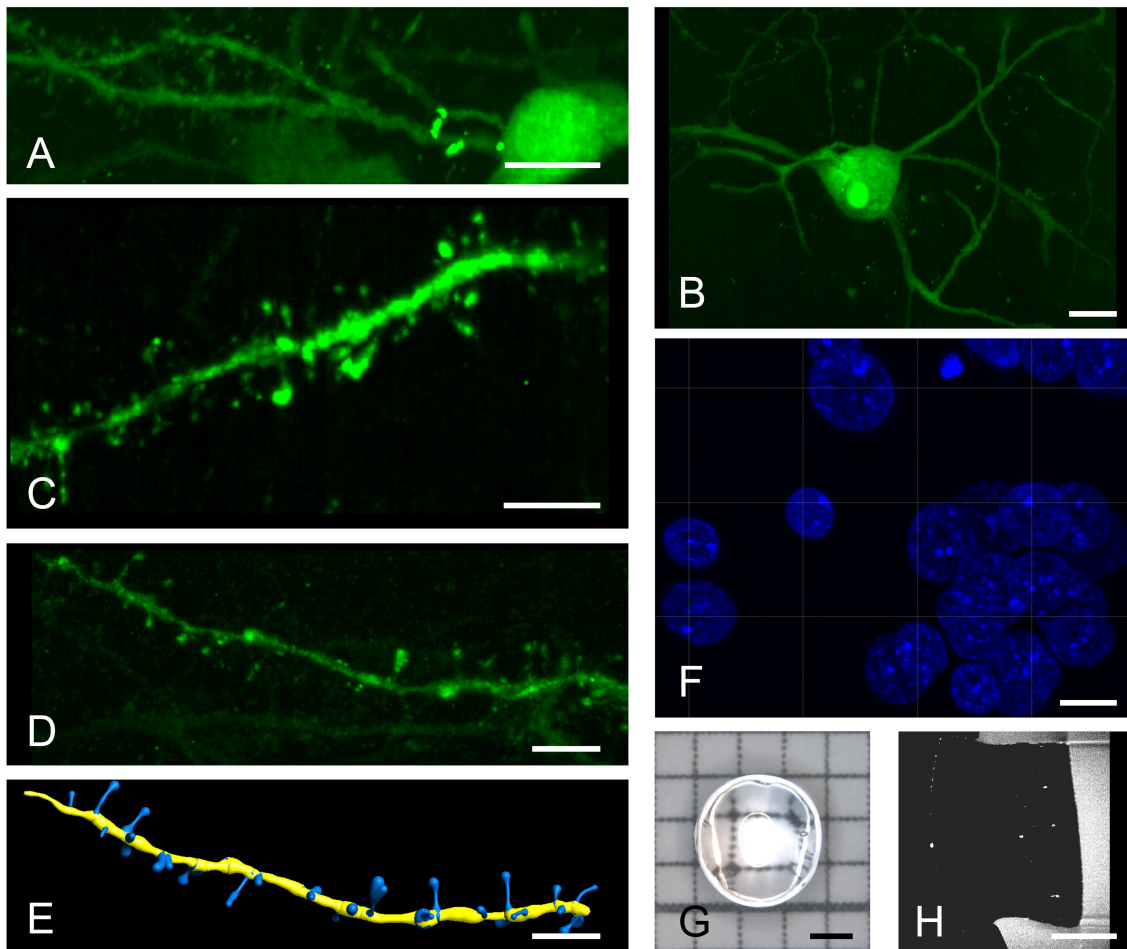


**FIGURE 2** | High resolution imaging of spiny and aspiny neurons. Top row shows a spiny (**A**) and an aspiny (**B**) neuron in Area X. Higher magnifications reveal distinct spine morphologies (**C,D**) that can be automatically quantified using the IMARIS filament tracer (**E**). A brief post-expansion DAPI staining (**F**) resolves cellular nuclei with labeled chromatin structures. We imaged 3 mm punch-outs (**G,H**) of 4-fold expanded, 60–100  $\mu\text{m}$  thick (pre-expansion) sagittal brain sections containing almost the entire Area X. All images are produced with a 20x, 1.0 NA water dipping objective. Scale bars (**A,B**)  $10 \mu\text{m}$ , (**C–F**)  $5 \mu\text{m}$ , (**G,H**)  $1 \text{ mm}$ . Scale bars in (**A–F**) correspond to pre-expansion dimensions.

## Ultramicroscope II for Large Samples

Figures 1G–I and Supplementary Movie S1 show a volume rendering of a tissue block with pre-expansion dimensions of  $[2500 \times 2000 \times 800] \mu\text{m}^3$ . Somata of HVC neurons are easily identifiable and axonal structures can be recognized even at low magnification (Supplementary Figure S2). Under increased magnification, fine structures such as spines can be discerned (Figures 1J,K).

## Z.1 for High Resolution Imaging

For analysis requiring higher resolution, we turned to a system that is equipped with regular microscope objectives. Images acquired with a 20x objective distinctly show surface structures of somata and dendrites in both spiny (Figure 2A) and aspiny (Figure 2B) neurons, which can be easily discriminated. Digitally zoomed-in maximum intensity projections of diverse dendrite fragments clearly reveal spines (Figures 2C,D) of distinct

morphologies (Figure 2E). General morphology and a spine density of  $0.70 \pm 0.09$  ( $n = 6$ ) per  $\mu\text{m}$  dendrite length match previous descriptions of HVC-X projecting neurons using EM (Kornfeld et al., 2017).

Post-expansion staining with DAPI shows exceptional details of the nucleus (Figure 2F) with image quality exceeding that of cell cultures imaged with gSTED (Okada and Nakagawa, 2015). We typically imaged 3 mm punch-outs of expanded sagittal brain sections of Area X (Figures 2G,H).

## DISCUSSION

We demonstrated the clearing capacities of our expansion protocol and showed that ExLSM allows for imaging of large volumes of brain tissue at subcellular resolution. In the following, we compare our approach to other clearing approaches. For a more in-depth review of cleared-sample imaging, we refer to Richardson and Lichtmann (2015, 2017) and to Silvestri et al. (2016); for a focus on clearing of songbird tissue, we refer to our other publication in the same research topic (Rocha et al., 2019).

### Transparency and Large Volume Imaging

A general limitation of light-based imaging techniques such as confocal microscopy is the increase in light scattering with tissue depth when imaging non-cleared specimens. The increase in background noise makes imaging at depths larger than  $50 \mu\text{m}$  impractical. Homogenization of refractory indices (RIs) across sample, embedding medium, and imaging medium is one common goal to all clearing methods (Silvestri et al., 2016). With ExLSM, commonly no tissue outlines are visible and gels themselves are completely transparent in water, which hints toward a near perfect match of RIs throughout the optical path. High tissue clarity is suggested by the extremely low levels of background light. Another advantage of water as imaging medium over solutions with different RIs is compatibility with imaging objectives, because no additional corrections in the imaging path are necessary.

Although we demonstrated the unobstructed imaging of cleared gel blocks of roughly one cubic centimeter, we emphasize that our gels contained biologically relevant data within only  $2 \text{ mm}^3$  pre-expansion. Whether the expansion and excellent clearing of much larger volumes is feasible remains to be tested.

Another factor to consider when imaging cleared tissue in a light sheet microscope is the color of the fluorophore. Because light of longer wavelength is less affected by scattering, the use of red fluorophores is generally advised, such as DRAQ5 as a nuclear marker instead of DAPI (Marx, 2016). Here, we demonstrated the compatibility of ExLSM with short-wavelength fluorophores.

### Retention of Native Fluorescence and Antigenicity

In general, organic solvent-based clearing methods do not preserve native fluorescence of proteins well, with the exception of uDISCO (Pan et al., 2016). GFP fluorescence is usually

well preserved, but we want to draw attention to the fact that the common model for assessing fluorescence preservation, the Thy-1 mouse line, has an exceptionally strong GFP signal (Dodt et al., 2007; Silvestri et al., 2016). Many protocols are to some degree compatible with antibody staining, but antibody penetration based on passive diffusion can take weeks (Richardson and Lichtmann, 2015). Additional usage of electrophoresis such as in CLARITY (Chung et al., 2013) or in PARS (Yang et al., 2014), or the use of pressure as in ACT-PRESTO (Lee et al., 2016) can accelerate antibody penetration, but these enhancements can be difficult to set up or expensive to use when turning to a commercial solution such as X-CLARITY™ (Logos Biosystems, South Korea). Expansion microscopy, on the other hand, allows for post-expansion staining and is readily compatible with a large number of genetically expressed fluorescent proteins and commercially available antibodies (Chozinski et al., 2016; Ku et al., 2016; Tillberg et al., 2016).

To stain in expanded tissues is a potentially very powerful advantage. By stretching and unfolding, proteins' epitopes may become more accessible (Alon et al., 2018), which can accelerate antibody penetration and increase labeling strength.

### Image Resolution

One important consideration for imaging is resolution. In light sheet microscopy, axial resolution is directly proportional to the physical thickness of the light sheet and lateral resolution depends on the imaging objective. When pushing the physical limits, bessel beam-based systems and lattice light sheets present the current pinnacle of high axial resolution with voxel sizes of  $150 \times 150 \times 280 \text{ nm}$  (Chen et al., 2014), but at the cost of smaller working distances associated with the high NA illumination and imaging objectives used.

Desired resolution is of course dependent on the scientific question at hand. Hence, the  $4\text{--}5 \mu\text{m}$  axial resolution that is achievable with conventional illumination lenses might be sufficient and even favorable for the sake of working distance. For example, considering the Nyquist criterion, isotropic resolution of  $5 \mu\text{m}$  is enough to resolve cell bodies with a diameter larger than  $10 \mu\text{m}$ , which is generally the case when looking at neurons. Although some clearing approaches can visualize dendritic spines in 2D with higher NA imaging objectives (Dodt et al., 2007), quantification of structure in 3D remains challenging. Even the recent addition to the CUBIC protocol, CUBIC-X (Murakami et al., 2018), that exploits the intermediate expansion of the protocol's reagent-1 to achieve a final 2-fold increase in volume, does not seem to allow for the distinct differentiation of spine morphologies (compare Figure 2H in Murakami et al., 2018).

We demonstrate that spine morphology can be quantified with ExLSM in a Zeiss Z.1 light sheet microscope with results comparable to conventional slice-based confocal microscopy, with the advantage of increased imaging speed. Whereas, imaging a volume of  $[100 \times 100 \times 10] \mu\text{m}^3$  takes minutes in a confocal microscope, the same volume of  $[400 \times 400 \times 40] \mu\text{m}^3$  is imaged in seconds with ExLSM

at a comparable resolution (Supplementary Figure S3). Considering a working distance of 2.4 mm for the 20x, 1.0 NA water-dipping objective used here, even quantification of spine morphologies in about 2 mm post-expansion sections is possible (corresponding to a native thickness of 500  $\mu\text{m}$ ).

## CONCLUSION

We have demonstrated the viability of expansion microscopy in the context of cleared large volume tissue imaging. The extremely short, easy, and inexpensive pre-processing in combination with great preservation of endogenous fluorescence, the possibility for post-staining, and its scalability make ExLSM a candidate for volumetric fluorescence imaging. We hope that this study encourages other labs to adapt our ExLSM approach to make imaging of large cleared and expanded volumes of brain tissue common practice in neural circuit analyses.

## DATA AVAILABILITY STATEMENT

Datasets are Available online at: <https://figshare.com/s/11103cff90436aa22630>.

## REFERENCES

- Alon, S., Huynh, G. H., and Boyden, E. S. (2018). Expansion microscopy: enabling single cell analysis in intact biological systems. *FEBS J.* doi: 10.1111/febs.14597. [Epub ahead of print].
- Bolhuis, J. J., Okanoya, K., and Scharff, C. (2010). Twitter evolution: converging mechanisms in birdsong and human speech. *Nat. Rev. Neurosci.* 11, 747–759. doi: 10.1038/nrn2931
- Bucur, O., Zhao, Y., Boyden, E., and Beck, A. H. (2016). Physical expansion of tissue microarrays for high-resolution imaging of normal and cancer samples with conventional microscopy. *Cancer Res.* 76. doi: 10.1158/1538-7445.AM2016-4229
- Cahoon, C. K., Yu, Z., Wang, Y., Guo, F., Unruh, J. R., Slaughter, B. D., et al. (2017). Superresolution expansion microscopy reveals the three-dimensional organization of the *Drosophila* synaptonemal complex. *Proc. Natl. Acad. Sci. U.S.A.* 114, E6857–E6866. doi: 10.1073/pnas.1705623114
- Chen, B. C., Legant, W. R., Wang, K., Shao, L., Milkie, D. E., Davidson, M. W., et al. (2014). Lattice light-sheet microscopy: imaging molecules to embryos at high spatiotemporal resolution. *Science* 346:1257998. doi: 10.1126/science.1257998
- Chen, F., Tillberg, P. W., and Boyden, E. S. (2015). Expansion microscopy. *Science* 347, 543–548. doi: 10.1126/science.1260088
- Chen, F., Wassie, A. T., Cote, A. J., Sinha, A., Alon, S., Asano, S., et al. (2016). Nanoscale imaging of RNA with expansion microscopy. *Nat. Methods* 13, 679–684. doi: 10.1038/nmeth.3899
- Chozinski, T. J., Halpern, A. R., Okawa, H., Kim, H. J., Tremel, G. J., Wong, R. O., et al. (2016). Expansion microscopy with conventional antibodies and fluorescent proteins. *Nat. Methods* 13, 485–488. doi: 10.1038/nmeth.3833
- Chung, K., and Deisseroth, K. (2013). CLARITY for mapping the nervous system. *Nat. Methods* 10, 508–513. doi: 10.1038/nmeth.2481
- Chung, K., Wallace, J., Kim, S. Y., Kalyanasundaram, S., Andalman, A. S., Davidson, T. J., et al. (2013). Structural and molecular interrogation of intact biological systems. *Nature* 497:332. doi: 10.1038/nature12107
- Doty, H. U., Leischner, U., Schierloh, A., Jährling, N., Mauch, C. P., Deininger, K., et al. (2007). Ultramicroscopy: three-dimensional visualization

## AUTHOR CONTRIBUTIONS

All authors conceived of the study. MG and RH provided instruments, materials, and reagents. DD, MR, and FD contributed to experiments, imaging, and interpretation of results. DD generated all figures. DD and MR wrote the first draft of the manuscript. All authors contributed to manuscript revision and read and approved the submitted version.

## ACKNOWLEDGMENTS

This work was supported by the European Union's Horizon 2020 Marie Skłodowska-Curie grant nr. 750055 to DD and ETH Grant ETH-42 15-1 to RH. Part of the imaging was performed at the Center for Microscopy and Image Analysis, University of Zurich. We thank Jean-Charles Paterna and Melanie Rauch of the Viral Vector Facility (VVF) of the Neuroscience Center Zurich (ZNZ) for AAV production.

## SUPPLEMENTARY MATERIAL

The Supplementary Material for this article can be found online at: <https://www.frontiersin.org/articles/10.3389/fnana.2019.00002/full#supplementary-material>

- of neuronal networks in the whole mouse brain. *Nat. Methods* 4:331. doi: 10.1038/nmeth1036
- Hahnloser, R. H., Kozhevnikov, A. A., and Fee, M. S. (2002). An ultra-sparse code underlies the generation of neural sequences in a songbird. *Nature* 419, 65–70. doi: 10.1038/nature00974
- Huang, Z., Khaled, H. G., Kirschmann, M., Gobes, S. M., and Hahnloser, R. H. (2018). Excitatory and inhibitory synapse reorganization immediately after critical sensory experience in a vocal learner. *Elife* 7:e37571. doi: 10.7554/eLife.37571
- Karagiannis, E. D., and Boyden, E. S. (2018). Expansion microscopy: development and neuroscience applications. *Curr. Opin. Neurobiol.* 50, 56–63. doi: 10.1016/j.conb.2017.12.012
- Kasthuri, N., Hayworth, K. J., Berger, D. R., Schalek, R. L., Conchello, J. A., Knowles-Barley, S., et al. (2015). Saturated reconstruction of a volume of neocortex. *Cell* 162, 648–661. doi: 10.1016/j.cell.2015.06.054
- Kleinfeld, D., Bharioke, A., Blinder, P., Bock, D. D., Briggman, K. L., Chklovskii, D. B., et al. (2011). Large-scale automated histology in the pursuit of connectomes. *J. Neurosci.* 31, 16125–16138. doi: 10.1523/JNEUROSCI.4077-11.2011
- Kornfeld, J., Benezra, S. E., Narayanan, R. T., Svava, F., Egger, R., Oberlaender, M., et al. (2017). EM connectomics reveals axonal target variation in a sequence-generating network. *Elife* 6:e24364. doi: 10.7554/eLife.24364
- Ku, T., Swaney, J., Park, J. Y., Albanese, A., Murray, E., Cho, J. H., et al. (2016). Multiplexed and scalable super-resolution imaging of three-dimensional protein localization in size-adjustable tissues. *Nat. Biotechnol.* 34, 973–981. doi: 10.1038/nbt.3641
- Lee, E., Choi, J., Jo, Y., Kim, J. Y., Jang, Y. J., Lee, H. M., et al. (2016). ACT-PRESTO: rapid and consistent tissue clearing and labeling method for 3-dimensional (3D) imaging. *Sci. Rep.* 6:18631. doi: 10.1038/srep18631
- Marblestone, A. H., Daugharthy, E., Kalhor, R., Peikon, I., Kechschull, J., Shipman, S., et al. (2013). Connectomics: the economics of large-scale neural connectomics. *bioRxiv* 001214. doi: 10.1101/001214
- Marx, V. (2016). Optimizing probes to image cleared tissue. *Nat. Methods* 13, 205–209. doi: 10.1038/nmeth.3774
- Murakami, T. C., Mano, T., Saikawa, S., Horiguchi, S. A., Shigeta, D., Baba, K., et al. (2018). A three-dimensional single-cell-resolution whole-brain atlas using

- CUBIC-X expansion microscopy and tissue clearing. *Nat. Neurosci.* 21:625. doi: 10.1038/s41593-018-0109-1
- Okada, Y., and Nakagawa, S. (2015). "Super-resolution imaging of nuclear bodies by STED microscopy," in *Nuclear Bodies and Noncoding RNAs* eds S. Nakagawa and T. Hirose (New York, NY: Humana Press), 21–35. doi: 10.1007/978-1-4939-2253-6\_2
- Pan, C., Cai, R., Quacquarelli, F. P., Ghasemigharagoz, A., Loubopoulos, A., Matryba, P., et al. (2016). Shrinkage-mediated imaging of entire organs and organisms using uDISCO. *Nat. Methods* 13, 859–867. doi: 10.1038/nmeth.3964
- Renier, N., Wu, Z., Simon, D. J., Yang, J., Ariel, P., and Tessier-Lavigne, M. (2014). iDISCO: a simple, rapid method to immunolabel large tissue samples for volume imaging. *Cell* 159, 896–910. doi: 10.1016/j.cell.2014.10.010
- Richardson, D. S., and Lichtmann, J. W. (2015). Clarifying tissue clearing. *Cell* 162, 246–257. doi: 10.1016/j.cell.2015.06.067
- Richardson, D. S., and Lichtmann, J. W. (2017). SnapShot: tissue clearing. *Cell* 171, 496–496. doi: 10.1016/j.cell.2017.09.025
- Rocha, M. D., Düring, D. N., Bethge, P., Voigt, F. F., Hildebrand, S., Helmchen, F., et al. (2019). Tissue clearing and light sheet microscopy: imaging the unsectioned adult zebra finch brain at cellular resolution.
- Scharff, C., and Nottebohm, F. (1991). A comparative study of the behavioral deficits following lesions of various parts of the zebra finch song system: implications for vocal learning. *J. Neurosci.* 11, 2896–2913. doi: 10.1523/JNEUROSCI.11-09-02896.1991
- Silvestri, L., Costantini, I., Sacconi, L., and Pavone, F. S. (2016). Clearing of fixed tissue: a review from a microscopist's perspective. *J. Biomed. Opt.* 21:081205. doi: 10.1117/1.JBO.21.8.081205.
- Stelzer, E. H. (2015). Light-sheet fluorescence microscopy for quantitative biology. *Nat. Methods* 12, 23–26. doi: 10.1038/nmeth.3219
- Susaki, E. A., Tainaka, K., Perrin, D., Yukinaga, H., Kuno, A., and Ueda, H. R. (2015). Advanced CUBIC protocols for whole-brain and whole-body clearing and imaging. *Nat. Protoc.* 10, 1709–1727. doi: 10.1038/nprot.2015.085
- Susaki, E. A., and Ueda, H. R. (2016). Whole-body and whole-organ clearing and imaging techniques with single-cell resolution: toward organism-level systems biology in mammals. *Cell Chem. Biol.* 23, 137–157. doi: 10.1016/j.chembiol.2015.11.009
- Tillberg, P. W., Chen, F., Piatkevich, K. D., Zhao, Y., Yu, C. C. J., English, B. P., et al. (2016). Protein-retention expansion microscopy of cells and tissues labeled using standard fluorescent proteins and antibodies. *Nat. Biotechnol.* 34, 987–992. doi: 10.1038/nbt.3625
- Tomer, R., Ye, L., Hsueh, B., and Deisseroth, K. (2014). Advanced CLARITY for rapid and high-resolution imaging of intact tissues. *Nat. Protoc.* 9, 1682–1697. doi: 10.1038/nprot.2014.123
- Vicario, D. S. (1991). Organization of the zebra finch song control system: functional organization of outputs from nucleus robustus archistriatalis. *J. Comp. Neurol.* 309, 486–494. doi: 10.1002/cne.903090405
- Yang, B., Treweek, J. B., Kulkarni, R. P., Deverman, B. E., Chen, C. K., Lubeck, E., et al. (2014). Single-cell phenotyping within transparent intact tissue through whole-body clearing. *Cell* 158, 945–958. doi: 10.1016/j.cell.2014.07.017
- Zhao, Y., Bucur, O., Irshad, H., Chen, F., Weins, A., Stancu, A. L., et al. (2017). Nanoscale imaging of clinical specimens using pathology-optimized expansion microscopy. *Nat. Biotechnol.* 35, 757–764. doi: 10.1038/nbt.3892

**Conflict of Interest Statement:** The authors declare that the research was conducted in the absence of any commercial or financial relationships that could be construed as a potential conflict of interest.

Copyright © 2019 Düring, Rocha, Dittrich, Gahr and Hahnloser. This is an open-access article distributed under the terms of the Creative Commons Attribution License (CC BY). The use, distribution or reproduction in other forums is permitted, provided the original author(s) and the copyright owner(s) are credited and that the original publication in this journal is cited, in accordance with accepted academic practice. No use, distribution or reproduction is permitted which does not comply with these terms.